Structural Dimensions and Their Changes in a Reentrant Hexagonal-Lamellar Transition of Phospholipids

R. P. Rand and N. L. Fuller
Department of Biological Sciences, Brock University, St. Catharines, Ontario, Canada

ABSTRACT A hexagonal-lamellar-hexagonal (H_{II}-L-H_{II}) reentrant phase transition sequence on dehydration of dioleoylphosphatidylethanolamine occurs below 22°C. This provides an unusual opportunity to measure how several structural dimensions change during this transition. Using x-ray diffraction, we have measured these dimensions with a hope of gaining some clue about the accompanying internal stresses. The principal dimensions described are molecular areas and molecular lengths projected onto the hexagonal lattice. In contrast with large changes in average area at the polar and hydrocarbon ends of the molecule, a position near the polar group/hydrocarbon interface is one of constant molecular area. It remains constant both as the monolayers curl from changing water content and in the transition from one structure to the other. In the L-to-H_{II} transition, the most obvious change in molecular length is a 25% decrease in the distance between aqueous cylinders, the interaxial direction. There is little change in the interstitial direction, the direction toward the interstice equidistant from three aqueous cylinders. As the hexagonal phase is dehydrated, a number of internal changes in molecular lengths are described. Increases in the interaxial direction are much larger than in the interstitial. Simultaneously however, hydrocarbon chain lengths decrease, and polar group lengths increase. It is likely that molecules move axially and the cylinders become longer with dehydration. These dimensions and their changes might be used in the search for a better understanding of the energetics of molecular packing, of the interpretation of spectroscopic measurements of these phases, and of the mechanics of lipid layers.

INTRODUCTION

Biological membranes contain lipids which, on their own, form non-bilayer structures. What role or effect such lipids have when constrained to planar membranes continues to be the subject of much speculation. Expectations are that non-bilayer-prone lipids would introduce perturbations or packing stresses within bilayers that affect the binding and conformation of membrane proteins. Such lipids may also facilitate the major conformational change required by fusogenic proteins. All fusion models require some high curvature and non-bilayer contortions of lipid packing, at least during the formation of a fusion pore. Ultimately an understanding of the energetics of lipid assemblies, and of the transitions between bilayer and non-bilayer assemblies, will be required to understand any such molecular interactions and transformations within membranes.

Two of the most common and much-studied assemblies, shown in Fig. 1, are the multibilayer lamellar (L) phase and the reverse hexagonal (H_{II}) phase (for a recent comprehensive review see Seddon, 1990). The simple symmetry and dimensions of these two structures belie an underlying complexity of factors contributing to their free energy and to transitions between them. The hexagonal versus lamellar packing has been understood tautologically in terms of "molecular shape," originally described by Luzzati and coworkers (Luzzati and Husson, 1962; Luzzati, 1968) and later formulated by a dimensionless parameter, $V/A \cdot l$, where V is the molecular volume, A the molecular area on the lipid-water interface, and l is the hydrocarbon chain length (Israelachivili et al., 1980). In more recent attempts to go beyond that tautology, the concept of spontaneous monolayer curvature (Helfrich, 1973) has translated the shape concept into terms of the balance of in-plane or lateral molecular interactions (Gruner, 1989). Transitions such as the L-to-H_{II} transition which involve large geometrical changes have been described in terms of curvature and other competing free energies of the system (Kirk et al., 1984; Kirk and Gruner, 1985). One of the latter is the chain stress required to populate the different environments around the axes of the hexagonal cylinder. Altogether, when interpreted beyond the narrow context of the steric shape of a rigid molecule, to include likely interactions such as polar group hydration or charge repulsion and a variety of chain conformations, such ideas have usually accounted for most observed phase transitions (Seddon, 1990).

Given this success, it was surprising and instructive to find two examples that so obviously contradict prediction. It has been observed recently that dioleoylphosphatidylethanolamine (DOPE) undergoes a reentrant H_{II}-to-L-to-H_{II} phase transition sequence on progressive dehydration (Gawrisch et al., 1992). The H_{II}-to-L transition in particular, which had also been seen in one earlier study (Boni et al., 1984), contradicts the otherwise universal observation that water removal reduces polar group area and induces the transition to the curved surfaces of the H_{II} phase. Worse, a measure of the osmotic work required to induce the H_{II}-to-L transition is about 5 to 10 times smaller than that estimated to unbend the H_{II} monolayers (Rand et al., 1990; Kozlov and Winterhalter, 1991b). Where the additional free energy becomes available during the transition is quite unresolved (Gawrisch et al.,

Received for publication 19 January 1994 and in final form 16 March 1994.
Address reprint requests to Dr. Peter Rand, Department of Biological Sciences, Brock University, St. Catharines, Ontario L2S 3A1, Canada. Tel.: 416-688-5550; Fax: 416-688-1855; E-mail: rrand@spartan.ac.brocku.ca.

0006-3495/94/06/2127/12 $2.00

V_l = volume of one phospholipid molecule

V_w = volume of water per phospholipid molecule

V_p = volume of the polar part

V_{hc} = volume of the hydrocarbon chains

$$\phi_l = \text{volume fraction of the non-aqueous part of the sample} = \frac{V_l}{V_w + V_l}$$

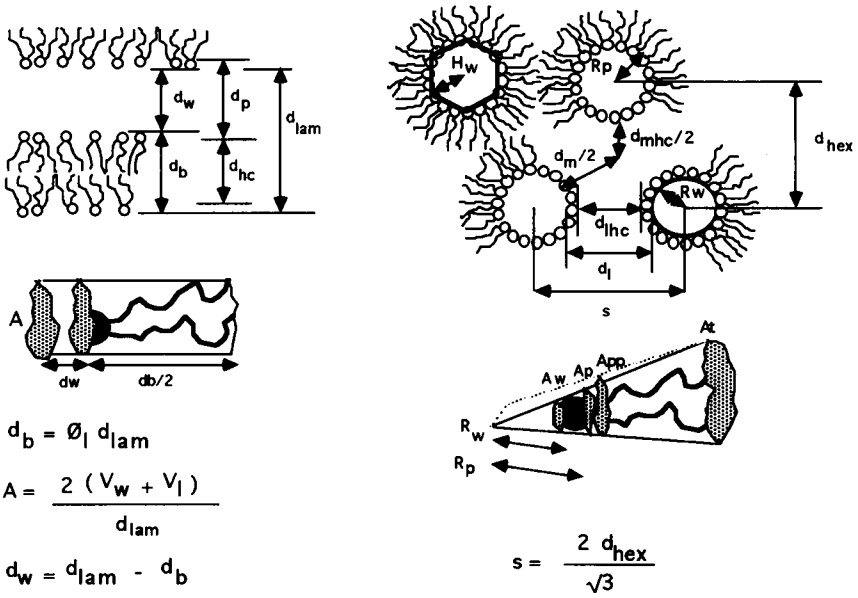

FIGURE 1 Schematic diagrams of the lamellar and hexagonal phases. Formulae for the derivation of the indicated structural parameters are shown. The text more fully describes the explicit meaning of these dimensions.

$$d_b = \phi_l\, d_{lam}$$

$$A = \frac{2\,(V_w + V_l)}{d_{lam}}$$

$$d_w = d_{lam} - d_b$$

$$d_p = \frac{2\,(V_w + V_p)}{A}$$

$$d_{hc} = \frac{2V_{hc}}{2}$$

$$s = \frac{2\,d_{hex}}{\sqrt{3}}$$

$$R_w^2 = \frac{2\,d_{hex}^2\,(1 - \phi_l)}{\pi\sqrt{3}} \quad \text{or} \quad H_w^2 = R_w^2\,\frac{2\pi}{3\sqrt{3}}$$

$$d_l = s - 2R_w \quad \text{or} \quad d_l' = s - \sqrt{3}\,H_w$$

$$d_m = 2\left(\frac{s}{\sqrt{3}} - R_w\right) \quad \text{or} \quad d_m' = 2\left(\frac{s}{\sqrt{3}} - H_w\right)$$

$$A(R) = \frac{\sqrt{3}\,\pi\,R\,V_l}{d_{hex}^2\,\phi_l} = \text{area available per lipid molecule, of volume } V_l, \text{ on the surface of a cylinder of radius R.}$$

1992). Finally, while charged lipids extend the lamellar phase region (Lerche et al., 1991), both hydrophilic molecules (Wistrom et al., 1989) and hydrocarbon molecules (Gawrisch et al., 1992) separately eliminate the reentrant transition. While the transition sequence has been accounted for on the basis of overall measured energetics, what the individual contributions are to the overall free energy of these lipid assemblies remains unclear (Gawrisch et al., 1992).

In addition to these new problems and in spite of the assault on the hexagonal phase itself by many methods, some basic questions about it persist. These also will require a better understanding of its internal free energies. Why do the molecules pack at very high curvature around the cylinder axis but with no curvature along the cylinder axis? What are the dynamic consequences of this structural anisotropy? While this geometry is consistent with minimizing the packing frustration of the system in terms of overall curvature (Charvolin, 1990), what free energies contribute to such minimization? The structural parameters described here reflect the time average of a variety of molecular configurations. Spectroscopic methods, on the other hand, characterize molecular motions ranging, for example, from atomic bond vibrations (Hubner and Mantsch, 1991) to the orientational order parameter of the C-C bonds along the hydrocarbon

chains (Lafleur et al., 1990). How the results of these different approaches complement each other also remains difficult to determine. For example, the translation of the nuclear magnetic resonance order parameter into molecular lengths consistent with x-ray measurements is not straightforward (Thormond et al., 1993).

It is in this light that we have investigated in detail several structural dimensions, shown in Fig. 1, of the DOPE lamellar and hexagonal phases, particularly as they change in the H_{II}-L-H_{II} transition region. The sandwiching of the lamellar phase between two H_{II} regions in a simple two-component system provides a unique opportunity to determine the changes in molecular packing that accompany this transition. These changes in dimension should reflect internal stresses and hopefully provide clues where to look for free energy changes. Since this transition can be induced osmotically (Gawrisch et al., 1992), these structural data can be used in a number of ways to analyze free energy changes in this system (Kozlov et al., 1994).

We document many structural parameters and their changes for these two phases at all levels of hydration. The principal results show the following. 1) The monolayer pivotal position or neutral plane is close to the polar/hydrocarbon interface, slightly different than that found in our earlier studies (Rand et al., 1990). 2) In the L-to-H_{II} transition, the most obvious change in projected molecular length is a 25% decrease in the interaxial direction with little change in the interstitial direction. 3) On dehydration, projected hydrocarbon chain lengths decrease while the polar group thickness increases. It is likely that molecules move axially and the cylinders become longer as water is removed. 4) Molecular lengths are never greater than exist in the bilayer, suggesting that bilayer thinning is facile and thickening is not. 5) We discuss the futility of trying to translate these rather precisely determined dimensions into molecular "shapes" such as cones and taper-shaped molecules, even though it is presumably the anisotropy of these "shapes" that results in monolayers with such disparity in its two principal radii of curvature in the H_{II} phase.

MATERIALS AND METHODS

Sample preparation and composition

Synthetic L-α-dioleoylphosphatidylethanolamine (DOPE), purchased from Avanti Polar Lipids, Inc. (Birmingham, AL), was used without further purification. The lipid was checked for impurities by thin-layer chromatography and judged to be at least 98% pure.

The lipid was stored under nitrogen at −18°C until used. The lipid was hydrated by weighing the dry lipid and 2 mM TES buffer (pH 7.4) into small weighing bottles and equilibrated in the dark at room temperature for 48 h. No water loss was detected before mounting the hydrated lipid into x-ray sample holders at the equilibrating temperature. Each sample was combined with some powdered Teflon as an x-ray calibration standard and then sealed between mica windows 1 mm apart. X-ray diffraction was used to characterize the structures formed by the various lipid mixtures. The CuKα_1 line (λ = 1.540 Å), from a Rigaku rotating anode generator, was isolated using a bent quartz crystal monochromator, and diffraction patterns were recorded photographically using Guinier x-ray cameras operating in vacuo. Temperature was controlled with thermoelectric elements to approximately ±0.5°C.

All samples formed hexagonal and/or lamellar phases. A lamellar phase is characterized by a series of three to seven x-ray spacings in the ratios of the unit cell dimension, d_{lam} of 1, 1/2, 1/3, 1/4, etc. A hexagonal phase is characterized by x-ray spacings bearing ratios to the dimension of the first order, d_{hex}, of 1, $1/3^{1/2}$, $1/4^{1/2}$, $1/7^{1/2}$, $1/9^{1/2}$, $1/12^{1/2}$, etc. Some samples showed two populations of x-ray spacings, all of which could be indexed in a lamellar and hexagonal series, indicating the coexistence of two phases. Their relative abundance can be judged very approximately by the relative intensity of each population of x-ray reflections.

Phase structure

Molecular packing and electron density maps have provided the molecular arrangement within the L and H_{II} phases (Luzzati and Husson, 1962). Lamellar phases are formed by alternating layers of water and bimolecular phospholipid layers. H_{II} phases are two-dimensional hexagonal lattices formed by the axes of indefinitely long and parallel regular prisms. Water cores, centered on the prism axes, are lined with the lipid polar groups and the rest of the lattice is filled with the hydrocarbon chains. The cross-section of the prism must be hexagonal in shape at the hydrocarbon chain boundaries of the hexagonal lattice. On the other hand, the cross-sectional shape of the water core prism within that lattice is normally assumed to be circular. However, it has been shown that that cross-section can be significantly distorted from circularity (Turner and Gruner, 1991).

For a single hexagonal or lamellar phase of known composition, the lattice can be divided into compartments as shown in Fig. 2, each containing defined volume fractions of the lipid and water. This volume average division follows the method originally introduced by Luzzati (Luzzati and Husson, 1962) and depends only on a knowledge of the densities of the molecular components and on the assumption of their linear addition. The specific volumes of many phospholipids have been measured directly. Here DOPE and water have both been taken as 1.00. The specific volume of melted hydrocarbon chains of the lipids was derived as 1.17 cm^3/g. The lipid polar groups are defined as including all polar moieties including the carbonyls at the polar group ends of the attached fatty acid hydrocarbon chains (see Rand and Parsegian, 1989, for a detailed discussion of molecular densities). On this basis, the molecular weights, partial specific volumes, and molecular volumes were used to derive the structural dimensions for DOPE and are shown in Table 1.

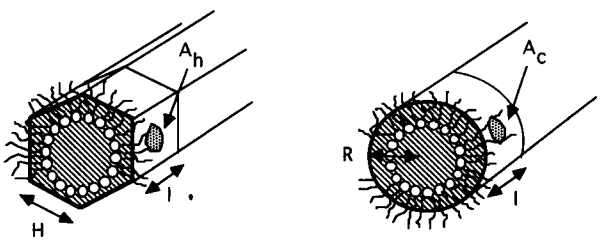

area of the right cross section of regular prisms

average area available per molecule on the surface of the dividing prism, containing fraction f of the volume of the lipid molecules,

$$A_c = 2 \cdot (V_W + f \cdot V_l)\ R$$

$$A_h = 4 \cdot (V_W + f \cdot V_l) / \sqrt{3} \cdot H$$

FIGURE 2 Schematic representation of the hexagonal phase divided into regular prisms centered on the axes of the aqueous compartment. The cross-sectional profiles of these prisms are either circular, of radius R, or hexagonal, of side H. According to the defined contents of these prisms, A_c and A_h give the average area available per molecule projected onto the surface of these prisms as described in the text.

TABLE 1 Structural dimensions of DOPE

Parameter	Mol. wt.	Partial specific volume	Volume (Å^3)
Lipid	740	1.00	1228
Polar group	269	0.671	312
Hydrocarbon chains	471	1.17	916

Based on the molecular packing as described above, molecular dimensions within the measured lattices are determined as described in Fig. 1. They are entirely consistent with measurements of similar dimensions defined from electron densities derived from the x-ray intensities (Turner and Gruner, 1991). A similar kind of analysis was undertaken (Scherer, 1989a) on previously published x-ray data of didodecylphosphatidylethanolamine (Seddon et al., 1984). However, as outlined below, it is important to recognize the limitations of these dimensions, particularly in attributing specific modes of molecular packing within them. That recognition should preclude over-interpretation of the ways in which these molecules pack in space (Gruner, 1989; Scherer, 1989b).

Molecular areas

Average molecular areas are one of the most precisely determined and useful structural parameters in these phases. Their determination requires only a knowledge of lattice dimension, sample composition, and molecular densities. It is important to recognize that they are independent of the structural resolution of the phase. This is shown in Figs. 1 and 2 and can be seen by considering a unit cell that contains one phospholipid molecule of volume V_l and the volume of water per lipid molecule, V_w, which is set by sample composition.

For a lamellar phase of repeat distance d as shown in Fig. 1, the average molecular area A available per phospholipid molecule in a plane parallel to the bilayer is $A = 2(V_l + V_w)/d$ and is constant throughout the lattice repeat distance d. The area is determined simply by the lattice dimension and sample composition.

For hexagonal structures the average molecular area, A, is that available to one lipid molecule on the surface of any defined regular prism parallel to the water core axis. The area at the axis is 0 and is strongly dependent on the distance of the defined prism surface, or dividing surface, from the axis, since that distance determines the fraction of the unit cell volume that is included within the prism. On the basis of the molecular arrangement within the hexagonal phase, we have determined the molecular area at various distances from the axis of the water cylinder. Turner and Gruner (1991) have provided evidence that the water core radius may deviate up to 10% from circularity. In treating this x-ray data we have chosen two extremes of profile, circular and hexagonal as shown in Figs. 1 and 2. The hexagonal profile itself represents a maximum variation of water "radius" of about 13%. The choice of profile has little effect on the derived dimensions and their trends.

The derivation of molecular areas is instructive in showing their meaning, precision, and limitations. Fig. 2 shows prisms that are either circular in cross-section and of radius R, or are hexagonal in cross-section and of side H. The prism surface of length l encloses V_w plus fraction f of the lipid volume V_l for each of n phospholipid molecules. Let the prism, of length l, be of cross-sectional area a_p and of circumference c_p. A is the area available per lipid molecule on the surface of the prism; then $la_p = n(V_w + fV_l)$ and $lc_p = nA$. Therefore, $A = (V_w + fV_l)c_p/a_p$. For the prism of circular cross-section of radius R, $c_p = 2\pi R$ and $a_p = \pi R^2$. For the prism of hexagonal cross-section of side H, $c_p = 6H$ and $a_p = H^2 \cdot 3^{3/2}/2$. For all prisms with the same contents, $n(V_w + fV_l)$, a_p is constant. Therefore the sizes of the circular and hexagonal prisms are related by $H^2 = R^2 \cdot 2\pi/3^{3/2}$. The molecular area on the surface of a circular prism is $A_c = 2(V_w + fV_l)/R$. The molecular area on the surface of a hexagonal prism is $A_h = 4(V_w + fV_l)/3^{1/2}H$, and $A_h/A_c = 1.05007$. Importantly then, molecular area requires only a measure of the lattice dimension and composition.

We assign A_t to the molecular area on the surface of the regular hexagonal prism, nominally occupied by the terminal ends of the hydrocarbon chains, defined by the whole lattice. A_w is the area at a lipid-water interface on the prism that would include all the water and no lipid. Molecular areas are calculated at intermediate positions by including within the prism a fraction f of the phospholipid molecular volume, taking into account the differential density of the polar and hydrocarbon parts of the molecule given above. A_p is the area on a prism that includes all the water and the polar group volume, i.e., at the polar group/hydrocarbon chain interface. Except for A_t which is uniquely determined because the cross-sectional shape of the prism is uniquely determined by the lattice, these areas are weakly dependent on the shape of the cross-section of the selected prism. We have calculated areas for both circular and hexagonal shapes, the latter of which, by geometry, are 5.007% larger.

Molecular length

For the lamellar phases the lattice dimension d is divided into partial thicknesses based on the partial volumes of the molecular constituents and according to the formulae of Fig. 1. d_l and d_w partition the lattice into two layers, one layer containing all the lipid and one layer containing all the water. d_p and d_{hc} partitions the lamellar repeat into a layer that contains all the water and polar groups and a layer that contains all the hydrocarbon chains, i.e., into a polar/hydrocarbon interface. The latter division circumvents the difficult problem of knowing the structure within the polar group/water region and defines what may be a less ambiguous interface.

For hexagonal phases equivalent partitioning to that described for the lamellar phase is made as shown in Fig. 1. s is the interaxial distance between the axes of the water cores. d_l is the "interaxial" "bilayer" thickness in the direction of the water core axes, and d_m is twice the distance, nominally two molecular lengths, from water core surface to the hexagonal interstice, the "interstitial" length. We have assumed that the water core prisms are either circular in cross-section and of radius R_w or are hexagonal in cross-section and of side H_w. As with the lamellar phase, we also partition the hexagonal phase into a polar core of radius R_p containing the water and polar groups and an exterior hydrocarbon space of dimension shown in Fig. 1. These linear dimensions depend, rather weakly, on the cross-sectional shape of the water core prism, as shown in Fig. 1, and unless otherwise stated we will refer to the circular case.

It is important to recognize that these derived molecular lengths are projections onto a plane. In the case of the lamellar phase, that plane is perpendicular to the plane of the bilayer, and in the case of the hexagonal phase that plane contains the right cross-section of the regular prism. It is usually assumed in these structures that the long axis of the molecules lies on average in these planes and that the derived lengths represent average molecular lengths. However, if on average, the long axis of the lipid molecule is tilted with respect to those planes, the derived lengths will be the projected component of the actual molecular length.

The absolute molecular dimensions and their changes are not determined uniquely by sample composition and geometry. For example, at any fixed sample composition in the hexagonal phase, the squares of the radius of the water cylinder R_w and the lattice spacing d_{hex} are related only by a constant (Fig. 1). But it is the minimization of free energy, depending on internal stresses, that determines the unique molecular packing and the absolute values of R_w and d_{hex}. Similarly, as the composition is changed, as water is added for example, the increase in lattice size depends on the relative increase in aqueous and lipid space. Therefore, dimensions d_m and d_l, for example, could change in a number of ways, the unique way being determined by how the system minimizes its free energy.

Relative contributions to changes in water content

A change in the water content of the hexagonal or of the lamellar phase can result from volume changes through two independent dimensions. One is a change in molecular area, and one is a change in the distance between polar group surfaces across the aqueous space. It is important to note that in both phases these two modes of volume change are independent, and the actual changes will be determined by how the system minimizes its

free energy. For example, in a lamellar phase whose bilayers were absolutely incompressible, all volume decrease would come from a decrease in interbilayer distance with no change in molecular area. In practice, bilayers are compressible and the division of the total volume change into those involving area changes and those involving changes of interbilayer distance led to measures of lateral compressibility and interbilayer repulsion (Parsegian et al., 1979).

We apply the same division of water volume change to these results. For the hexagonal phase $V_w = A_w R_w/2$ and $1/2\ \Delta V_w = A_w \Delta R_w + R_w \Delta A_w$, let $A_w \Delta R_w = \Delta V_R$, the volume change due to a change in R_w, and $R_w \Delta A_w = \Delta V_A$, the volume change due to a change in area. Then the ratio $\Delta V_R/\Delta V_A = A_w/R_w * \Delta R_w/\Delta A_w$.

Similarly for the lamellar phase, $\Delta V_{dw}/\Delta V_A = A/d_w * \Delta d_w/\Delta A$. These ratios then measure the relative contribution to the total change in water content of a change in the dimension of the aqueous space and of a change in molecular area. They can be derived from the measured relation between molecular area and either R_w or d_w. These ratios represent the relative work in effecting changes in molecular area and water distance.

RESULTS

The phase diagram

Fig. 3 shows the phase diagram of DOPE in 2 mM TES buffer, pH 7.4. Each data point is the result of separate x-ray diffractograms. These data are consistent with that published earlier (Tate and Gruner, 1989) but provide more detail, particularly in the lamellar phase region which itself was not reported. At temperatures above about 23°C a single hexagonal phase exists at all water contents. Below 23°C and in a restricted region around eight water molecules per phospholipid a single lamellar phase exists. On the higher water side, lamellar and hexagonal phases coexist between the single-phase regions. On the lower water side, a cubic phase exists in a very restricted region between the lamellar and hexagonal phases.

The hexagonal-lamellar-hexagonal reentrant phase transition sequence that occurs at lower temperatures as the water content is systematically changed is contrary to all experimental evidence, except one instance (Boni et al., 1984), that phospholipid H_{II} phases always have lower water content than adjacent lamellar phases (Seddon, 1990). However, we have discussed the energetics of this transition sequence and derived the qualitative aspect of this phase diagram (Gawrisch et al., 1992). This provoked us to investigate any differences between the hexagonal phases on either side of the lamellar phase and to inspect more closely the changes in internal dimensions that occur in the hexagonal-to-lamellar structural transition. We provide in Table 2 all our measured and derived molecular dimensions for the hexagonal phase at 22°C and as defined in Fig. 1. Readers may then deduce whatever relationships seem apparent.

Lattice dimensions

Fig. 4 shows the dimensions d_{hex} and d_{lam} at 22°C of the hexagonal and lamellar phases as the water content is changed. The very restricted region of single lamellar phase is seen at weight fraction water of about 0.18, or about eight or nine water molecules per lipid. The dimensions of the lamellar and hexagonal phases in their region of coexistence, and at all temperatures, are not significantly different from those of the single phases on either side.

Fig. 3 gives d_{hex} at the upper and lower extremes of temperature studied. The changes in dimension with temperature at any water content are not detectably different from those observed in other systems of lamellar and hexagonal phases. At the lower temperatures the hexagonal phases on either side of the lamellar phase show no unusual dimensions that

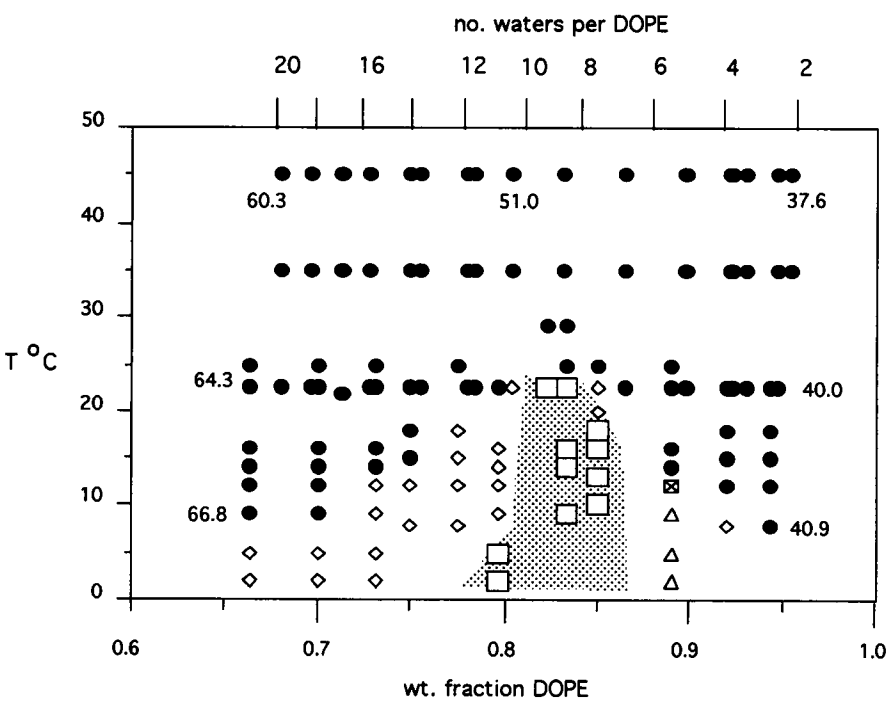

FIGURE 3 Phases formed by DOPE as a function of water content and temperature as determined by x-ray diffraction. The numbers give representative hexagonal spacings. The shaded block indicates the region of single lamellar phase. ●, hexagonal phase; □, lamellar phase; ◇, coexisting lamellar and hexagonal phases; ⊠, cubic phase; △, coexisting cubic and hexagonal phases.

TABLE 2 Hexagonal phase parameters for DOPE at ~22°C*

c	d_{hex} (Å)	V_w (Å^3)	n_w	R_w (Å)	R_p (Å)	d_l (Å)	d_m (Å)	d_{thc} (Å)	d_{mhc} (Å)	A_w (Å^2)	A_p (Å^2)	A_{pp} (Å^2)	A_t (Å^2)	n_c
0.947	40.2	69	2.3	5.6	13.2	35.2	42.4	20.0	27.1	24.5	57.8	62.5	111.8	11.4
0.943	40.0	75	2.5	5.8	13.2	34.6	41.8	19.7	26.9	25.7	58.6	63.3	112.8	11.3
0.930	40.7	93	3.1	6.5	13.7	33.9	41.2	19.6	26.9	28.3	59.4	63.9	112.4	11.6
0.924	40.5	101	3.4	6.8	13.7	33.2	40.5	19.3	26.6	29.9	60.5	65.0	113.7	11.5
0.922	41.3	104	3.5	7.0	14.0	33.7	41.1	19.7	27.0	29.7	59.6	64.0	111.8	11.8
0.920	41.8	107	3.6	7.2	14.2	33.9	41.4	19.8	27.3	29.8	59.1	63.5	110.7	12.0
0.898	43.6	140	4.7	8.4	15.2	33.5	41.2	19.9	27.7	33.1	59.6	63.7	108.7	12.8
0.890	43.9	152	5.1	8.8	15.5	33.0	40.9	19.8	27.6	34.4	60.2	64.3	108.9	12.9
0.864	47.0	194	6.5	10.5	17.0	33.3	41.7	20.2	28.6	36.8	59.6	63.3	104.8	14.3
0.797	53.7	314	10.5	14.7	20.8	32.7	42.3	20.5	30.1	42.7	60.4	63.4	99.4	17.2
0.785	54.4	338	11.3	15.3	21.3	32.2	41.9	20.3	30.0	44.0	61.2	64.1	99.7	17.5
0.780	54.6	348	11.6	15.5	21.4	32.0	41.7	20.2	29.9	44.6	61.6	64.5	99.9	17.5
0.776	56.0	356	11.9	16.1	22.1	32.5	42.5	20.5	30.6	44.1	60.6	63.4	97.9	18.2
0.755	58.0	400	13.3	17.4	23.3	32.2	42.5	20.4	30.8	45.8	61.2	63.9	97.2	19.1
0.750	58.6	411	13.7	17.8	23.6	32.1	42.6	20.5	30.9	46.1	61.3	63.9	96.8	19.3
0.749	59.5	413	13.8	18.1	24.0	32.6	43.2	20.7	31.4	45.6	60.5	63.1	95.5	19.8
0.732	60.9	452	15.1	19.1	24.9	32.1	43.0	20.5	31.4	47.1	61.3	63.8	95.5	20.4
0.727	61.7	463	15.4	19.5	25.3	32.2	43.2	20.6	31.6	47.2	61.2	63.7	94.9	20.7
0.713	62.2	496	16.5	20.2	25.8	31.4	42.5	20.2	31.3	49.0	62.6	65.0	96.0	20.9

* See Fig. 1 and text.

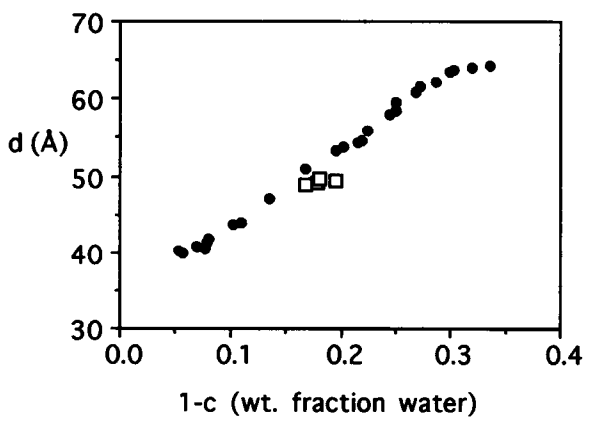

FIGURE 4 Lattice dimensions, d_{hex} and d_{lam}, for the phases formed by DOPE at 22°C as the water content is varied. ●, hexagonal phase; □, lamellar phase.

would indicate that they are any different than the higher temperature hexagonal phases at equivalent water content. This is consistent with our reconstruction of the phase diagram using the energetics of the two phases (Gawrisch et al., 1992).

The hexagonal phase at 22°C stops taking up water at 30 wt %, or 18 waters per lipid, beyond which excess water coexists with the hexagonal phase. We estimate this maximum hydration from the data as previously described (Gawrisch et al., 1992) and it agrees well with the value of 30.5% independently estimated from the electron density profiles of this lipid in excess water (Turner and Gruner, 1991). It is up to this level of hydration that the compositions of the single phases are defined and from which the molecular dimensions of Table 2 are derived. The lamellar phase has been estimated to take up water to the maximum extent of 9 or 10 waters per molecule.

Molecular areas

Fig. 5 shows the molecular areas of DOPE at 22°C as the water content is varied. For the hexagonal phases the average area at the terminal ends of the hydrocarbon chains, A_t, is uniquely determined. A_w and A_p are shown for a circular cross-section shape of the prism. Areas for a hexagonal cross-section would simply be higher by a constant 5%. The molecular area of DOPE in the interposing lamellar phase is also shown and is the same through the length of the molecule. There are three major variations in area which are noteworthy.

First, at any fixed water content there is a large difference in molecular area at each end of the molecule in the hexagonal phase. A_t/A_w varies from 2 to 5, depending on the water content. A_t/A_p varies by a factor of 2. So even within the hydrocarbon region itself there is twofold increase in molecular area in going from polar group end to methyl group end. These ratios are a good measure of a shape parameter, usually referred to as the "taper," "cone," or "wedge" shape of molecules packed into such highly curved surfaces.

Second, the transition from the lamellar to the hexagonal phase involves large internal changes in molecular area. In that transition the polar end of the molecule is compressed and the hydrocarbon end is dilated. For example, the chain terminals undergo a change from 60 to 120 Å^2, the polar group/water interface from 60 to 40 Å^2. However, at the polar/hydrocarbon interface, the hexagonal and lamellar areas differ very little.

Third, Fig. 5 shows that as the water content of the hexagonal phase is changed, molecular areas within the molecule can change in opposite directions. As we have shown previously (Rand et al., 1990), A_w decreases continuously on removing water, a change at the polar group end of the molecule that has been shown to occur for all phases. At the same

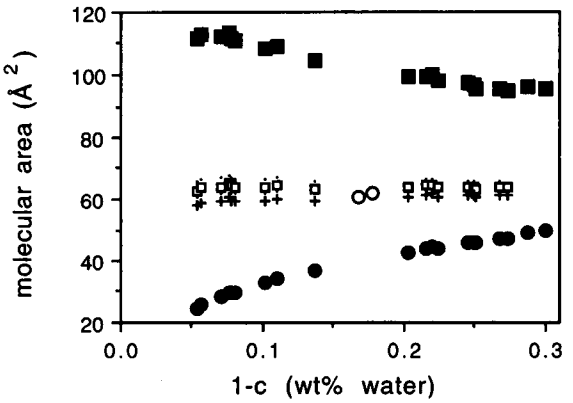

FIGURE 5 Molecular areas, as defined in the text, for the lamellar and hexagonal phases formed at 22°C as the water content is varied. ●: A_w, area at the water/lipid interface. +: A_p, area at the water plus polar group/hydrocarbon interface. ■: A_t, area at the boundaries of the unit cell, nominally the terminal ends of the hydrocarbon chains. □: A_{pp}, area at a position that includes all the water and lipid polar groups plus 0.074 of the volume of the hydrocarbon chains. The slope of these areas versus water content is not significantly different from 0. •: areas at positions that include 0.03 and 0.11 of the volume of the hydrocarbon chains as well as the water and polar groups. Slopes of these areas versus water content differ from 0 with a $p \approx 5\%$. ○: average molecular area for the lamellar phase.

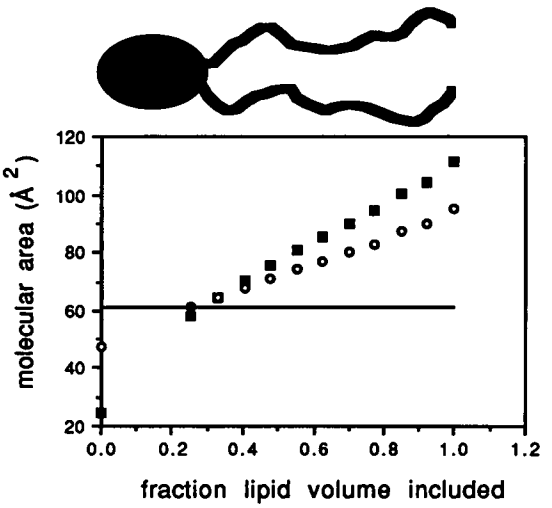

FIGURE 6 Average molecular areas available at different positions along the phospholipid molecule at two extremes of hydration of the hexagonal phase (■: $c = 0.95$; ○: $c = 0.73$) (Table 2). With dehydration polar group area decreases and hydrocarbon area increases. At a position that includes about 0.3 of the lipid molecule there is little detectable change in area with water content. The horizontal line indicates the molecular area of the intervening lamellar phase.

time, however, A_t increases. In this sense the molecule is compressed at the polar end and dilated at the hydrocarbon chain end of the molecule as the curvature of the monolayer surrounding the aqueous core is increased by removing water. A_t in particular reaches remarkably large values.

The area changes in the hexagonal phase suggest that there is a position within the molecule that remains constant in area as the water content is changed. Such a pivotal position and area, A_{pp}, for this DOPE was sought by determining molecular areas on the surfaces of prisms that enclose ever-increasing fractions f of the molecular volume. Fig. 5 includes the areas, A_{pp} at a position that includes all the water and the polar groups plus 7% (±4%) of the volume of the hydrocarbon chains. That range of hydrocarbon yields slopes of areas versus water contents that do not differ significantly from 0 ($p < 0.05$). This we define as the pivotal position or neutral plane of the monolayer.

The variation of molecular area with water content at various positions within the molecule can be seen more clearly in Fig. 6. At a position along the molecule that includes 31 ± 3% of the polar end of the molecular volume, the area changes least over the range of hydration studied. That position is, approximately, at the first carbon of the hydrocarbon chain. The horizontal line shows the molecular area in the lamellar phase.

This pivotal position is somewhat different from that initially reported in an earlier study in which the position was estimated to be at the third or fourth carbon of the chain (Rand et al., 1990). While these current data are more extensive, the statistical limits are close to each other and the total change in the areas within the ranges of slopes given by the statistical limits are of the order of the experimental errors. So, while the present data are considered to be more precise, it remains to be seen how sensitive this determination is with respect to different lipid preparations.

Number of molecules around the circumference

While these areas and their changes are quite precise, this measure of "compression" and "dilation" cannot be easily translated into molecular dimensional changes that occur around or along the cylinder axis. This is because there is no information about the number of molecules around the circumference of the cylinder and how that changes. Nevertheless, the molecular areas allow an estimate of these numbers and how they change on water removal. The circumferential number of molecules is $n_c = 2\pi R_w l/A_w$, where l would be the average length taken up by a molecule in a direction along the axis of the cylinder at the water-lipid interface. Taking the square root of the molecular area at the pivotal plane as an approximation of l gives the values of n_c shown in Fig. 7. On this basis the number of molecules around the circumference diminishes by a factor of 2 or 3 as water is removed, consistent with similar estimates for didodecylphosphatidylethanolamine (Scherer 1989). For n_c to remain constant as water is removed, l would have to change by more than 4 Å, highly unlikely for a molecule with average area of 60 Å^2. This suggests that molecules move longitudinally to lengthen the cylinder as the radius decreases.

Linear molecular dimensions

This section describes projected molecular lengths on the plane of the hexagonal lattice. While it is usually assumed

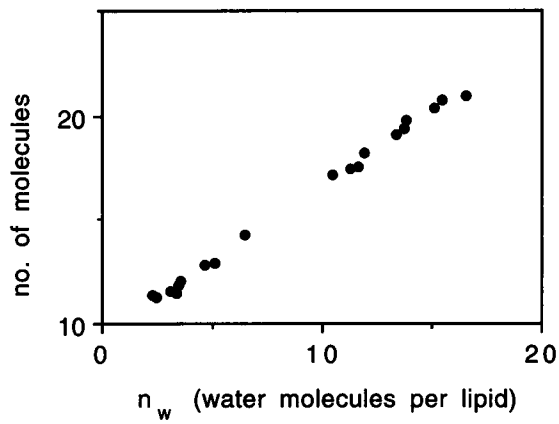

FIGURE 7 Estimates of the average number of molecules around the circumference of the aqueous channel as the number of water molecules per lipid, n_w, varies. These are estimated by assuming that the length that the molecules take up along the cylindrical axis is given by the square root of A_{pp}. As the lipid is dehydrated, circumferential numbers almost certainly go down and the cylinders lengthen.

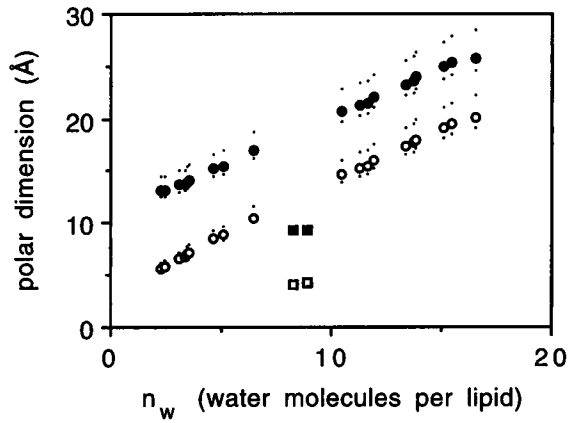

FIGURE 8 Polar dimensions of DOPE hexagonal and lamellar assemblies as they vary with number of water molecules per DOPE molecule. ○, water dimensions R_w; ●, water plus polar group dimensions R_p. The small symbols give the equivalent range of dimension assuming a hexagonal rather than circular cross-section of the polar prism. Squares give equivalent dimensions for the lamellar phase, $d_w/2$ and $d_p/2$. For the hexagonal phase these dimensions decrease with dehydration, and large changes in them occur on transition between lamellar and hexagonal phases. The distance of the farthest water molecule from the polar interface in the hexagonal phase is twice that of the lamellar phase.

that the molecules lie, on average, radially and in this plane, that assumption has not been established. Any tilt of the long axis of the molecule away from the radial direction or out of the lattice plane and toward the cylinder axis would give projected molecular lengths less than actual molecular lengths.

In excess water, the hexagonal dimensions derived here agree extremely well with those derived from electron density maps of DOPE (Turner and Gruner, 1991). Here particular attention is paid to the changes in dimension that result from water removal, and that occur in the transition from hexagonal to lamellar packing of the molecules. The dimensions in Table 2 are for prisms of circular cross-section. The trends and conclusions are little affected by assuming a prism of hexagonal cross-section. It is useful to divide the total changes in length into changes of the polar region and of the hydrocarbon chain region.

Polar region

Fig. 8 shows the radii of the polar group region, both a separate water cylinder, R_w, and a cylinder containing both water and polar groups, R_p. The maximum and minimum values for an equivalent hexagonal prism are shown for comparison. Both R_w and R_p increase linearly as the water content is increased up to maximum hydration.

Included in Fig. 8 is the equivalent dimension of the intervening lamellar phase, i.e., half of the interbilayer spacing. It shows that the hexagonal-to-lamellar phase transition results in a very large reduction in the distance from the polar group or hydrocarbon surface to the furthermost water region. The interbilayer spacing is one-half to one-third the water core diameter. The difference results because of the expansion in average area of the polar group region in the hexagonal-to-lamellar transition. It is important to recognize that this reduction is not fixed by geometry but rather by the

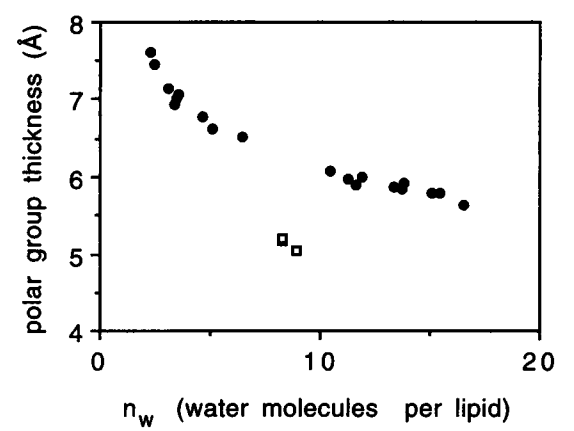

FIGURE 9 Variation of the nominal polar group thickness for the hexagonal (●) and lamellar (□) phases of DOPE with the number of water molecules per DOPE molecule. Polar group thinning is observed both with increasing hydration of the hexagonal phase and with its transition to the lamellar phase.

way the molecules, in minimizing their free energy, pack in the two phases. These results illustrate that there are large rearrangements in the polar group/water region in the phase transition. In particular, they suggest that with the formation of the hexagonal phase there is removal of water laterally from between polar groups and expansion of the water dimension in the direction toward the water axis, a lateral dehydration of polar groups.

The difference between R_p and R_w is the nominal polar group thickness. Fig. 9 shows a large relative decrease in polar group thickness with added water. This is analogous to the thinning of bilayers on hydration. The hexagonal-to-lamellar phase transition is accompanied by a thinning of this polar group layer.

"Bilayer" dimensions

Fig. 10 shows the "bilayer" dimensions in the hexagonal phase, i.e., the average length of two phospholipid molecules, both in the interaxial direction, d_l, and in the direction of maximum length, toward the interstices, d_m. Also shown are the dimensions of the hydrocarbon portions of those lengths. Although not so evident on the scale of Fig. 10, the slopes of all the lines, except as described below, are significantly different from 0 with $p > 99.9\%$. Several points are noteworthy: 1) The length in the interaxial direction, d_l, is about 25% less than d_m over most of the range of water contents. For a hexagonal prism that difference is about 15%. 2) As water is removed and the lattice size diminishes, d_l increases, d_m is nearly constant, and their difference systematically decreases. 3) As water is removed, the hydrocarbon length in the interstitial direction decreases considerably, while that in the interaxial direction decreases slightly but significantly. Assuming a uniform polar group dimension, within the total molecular dimension the polar group portion of that dimension increases, as shown in Figs. 9 and 10. 4) Equivalent thicknesses of the interposing lamellar phase are also shown in Fig. 10. They are the same as those in the interstitial direction and are significantly greater than those in the interaxial dimension of the hexagonal phase. This shows that the L-to-H_{II} transition results in significant shortening of the chains in the interaxial direction with little change in the direction toward the interstice. The particularly low values of d_l show that in the interaxial direction, and not in the interstitial direction, the molecules may be particularly highly splayed, may be interdigitated, or may be tilted toward the prism axis. 5) From the differences in dimension between the lamellar and hexagonal phases indicated in (4) above, one would estimate that the molecular area change that results on transition to the hexagonal phase, and discussed in the last section, would be greater in the interaxial direction than the interstitial.

With the exception of the projected molecular length in the interstitial direction, all these trends with dehydration are the same whether one assumes circular or hexagonal cross-section profile of the aqueous or polar prism. For that exception, the trend is in the opposite direction. However, in this case, the change is the smallest detected, ~1 Å. We take it that this dimension is particularly constant and maintains this maximum molecular length even in the bilayer.

Relative contributions to changes in V_w

A change in total water volume in the lamellar or hexagonal phase can be divided into a portion that involves a change in molecular area, A_w, and a portion that involves a change in d_w or in R_w. In Fig. 11 we have plotted, as a function of water content, the percentage of the total volume change that comes from a change in molecular area. The DOPE lamellar phase itself is constrained to too narrow a range of water contents to make those measurements. To compare phases in Fig. 11, we include data for an egg PC lamellar phase (Parsegian et al., 1979). For the lamellar phase, ~20% of the total volume change comes from a change in molecular area, and that proportion systematically decreases as the water content goes down. By contrast, in the hexagonal phase a higher proportion goes into area changes, is approximately constant until about 2/3 of the water is removed, and then increases sharply. This suggests that the polar groups in the hexagonal phase monolayers are relatively more compressible than in the bilayer.

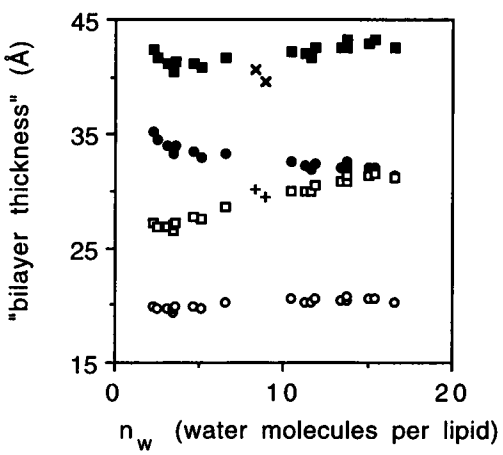

FIGURE 10 Variation of equivalent total bilayer and hydrocarbon thicknesses of the hexagonal and lamellar phases of DOPE with number of water molecules per DOPE molecule. ■, d_m; ●, d_l; □, d_{mbc}; ○, d_{lhc}; ×, lamellar d_l; +, lamellar d_{hc} (as illustrated in Fig. 1). The trends for the hexagonal phase are described in the text. The most obvious change in the L-to-H_{II} transition is the maintenance of molecular length in the interstitial direction and the significant shortening of the interaxial, total, and hydrocarbon thicknesses.

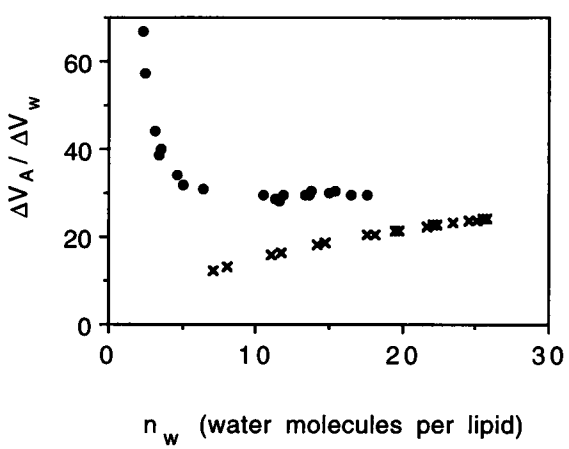

FIGURE 11 When a total volume of water ΔV_w is removed from the DOPE hexagonal phase, a proportion comes from decreasing the dimension of the water cylinder and a proportion from decreasing molecular area ΔV_A (see text). The latter presumably reflects the lateral compressibility of the monolayer relative to bending without area change. $\Delta V_A/\Delta V_w$ as a percentage is plotted as a function of the number of water molecules per DOPE molecule (●). Equivalent proportions are plotted for the lamellar phase of egg phosphatidylcholine (×). The trends are in opposite directions with the hexagonal phase showing a rapidly rising proportion at low water content.

DISCUSSION

Previously measured energetics of these structural changes suggested that the cost of flattening the H_{II} monolayer against its measured bending modulus was offset by some other competing free energies. With many possibilities for their source (Rand et al., 1990; Gawrisch et al., 1992) we were left with little understanding of the energetics of these phases. We hoped to gain some idea about the internal stresses in these structures by measuring the molecular dimensions of the H_{II} and L phases, since these dimensions are determined by how the system minimizes its free energy. Most recently (Kozlov et al., 1994) we have considered the H_{II}-L-H_{II} transition on the basis of a competition between curvature and hydration energy of the constituent monolayers.

The H_{II}-L-H_{II} transition

The major change in projected molecular length observed in the L-H_{II} transition is shortening in the interaxial direction, consistent with previous studies (Seddon et al., 1984), and near constant molecular length in the interstitial direction (Fig. 10). The bilayer thickness and twice the maximum molecular length, d_m, in the H_{II} phase are remarkably conserved in this transition. One way in which the system apparently minimizes its energy in the L-to-H_{II} transition is by, on average, molecular shortening and not by extension.

There are a number of ways that the hydrocarbon chain length could be reduced: the number of gauche rotamers may increase, the molecules may interdigitate, or the molecular axis may tilt away from the normal to the monolayer. Tilting might be detected using x-ray diffraction of oriented H_{II} cylinders. These possibilities for shortening are not mutually exclusive, nor easily distinguished, but presumably each might contribute differently to the free energy of the system. However that shortening occurs, one possibility is that a strong van der Waals attraction between aqueous cylinders (Parsegian, 1972) compresses, shortens, or bends the chains situated directly between them.

The maximum thickness, d_m, is maintained both as the hexagonal phase is dehydrated and in formation of the bilayer. Thickening requires lengthening of the hydrocarbon chains whereas "thinning" can be accomplished a number of ways as described above. One might expect on this basis that bilayer thickening would be more difficult than thinning. This consideration is relevant to models that consider the energetics of matching bilayer spanning peptides to lipid thicknesses and also to the mutual effects of lipid/protein interactions (see, for example, Fattal and Ben-Shaul, 1993).

Coupled to these changes in linear dimensions are the changes in molecular area. The average molecular area at the ends of the hydrocarbon chains in the H_{II} phase is nearly a factor of 2 larger than the areas of either the pivotal position or of the lamellar phase. That terminal area must be even greater in the interaxial direction and smaller in the interstitial direction as a result of their difference in molecular lengths. In any case, large changes in area in some parts of the molecule accompany the L-H_{II} phase transition.

Eventually one would like to understand all these changes in terms of the several contributions to the free energy of these structures. We earlier described the overall free energy conditions that are required for the re-entrant transition (Gawrisch et al., 1992). As a first step in trying to understand individual free energy contributions, we have treated the H_{II}-L-H_{II} transition itself, on a simple model that balances curvature energy of the H_{II} phase and hydration energy of the lamellar phase (Kozlov et al., 1994).

Changes within the H_{II} phase

Dehydration of the H_{II} phase itself is accompanied by changes in molecular lengths and areas. These changes may be different around the axis of the aqueous prism. The maximum molecular length in the interstitial direction remains approximately constant, i.e., it either increases or decreases by 1 Å depending on the chosen profile of the aqueous cross-section. It is as if, at all degrees of hydration, the molecules remain at some maximum fixed length, the same it has in the bilayer (Fig. 10), and fill the rest of the space at the whatever shorter lengths are required to fill the volume. On the other hand, the shorter average length in the interaxial direction increases by 4–5 Å. This difference in response to water removal presumably reflects the anisotropy in the different environments around the H_{II} prisms (Turner and Gruner, 1992, Turner et al., 1992).

The pivotal position

We have defined the pivotal position within the molecule, or a neutral plane within the monolayer, as that place which undergoes little change in area as the monolayer is bent. Importantly, the results show that the molecular area of that position coincides with the molecular area of the molecules when they assemble in the lamellar phase (Fig. 5).

Kozlov and Winterhalter (1991a, b) have defined a neutral plane by taking into account both bending and area extension deformations of the monolayer. Defined as that position where the modulus of mixed deformation vanishes, their neutral position is within an Ångstrom of that with constant area. More importantly, however, their analysis shows that derived elastic moduli defining those deformations depend sensitively on the choice of the dividing surface. This consideration becomes important for those studies that attempt to determine the energetics of formation of highly curved surfaces. One particularly interesting application of this is in the question of membrane fusion. The choice of what structural intermediates likely occur in the topological rearrangement during fusion (Seigel, 1993) is based on the energetics of those intermediates.

It is remarkable that there exists a position of constant area within the molecule as the monolayer is bent under changing composition. There is no a priori reason to assume either that such a position exists or that it be within the molecule itself. It can be different depending on how the curvature changes are induced. Analysis of data showing thermally induced

changes in curvature (Tate et al., 1992) places any such neutral position outside the molecule as expansion of both polar and hydrocarbon regions occurs.

In the present case, the pivotal position is very close to the boundary that separates the chemically distinct polar and hydrocarbon regions. Seen as a fulcrum that balances in-plane forces, one is led to believe that such different regions on each side of the fulcrum would be endowed with very different lateral and bending forces; the polar group side by polar group interactions including hydration, the apolar side by hydrocarbon chain interactions. The neutral position itself would be one of minimum compressibility. One might expect that lateral interactions on either side could act independently in affecting the curvature of the monolayer. In fact it is now known that either alkanes or small polar solutes prevent the formation of the lamellar phase of DOPE. Dodecane prevents formation of the lamellar phase (Gawrisch et al., 1992), trehalose stabilizes the DOPE H_{II} structure, contrary to its original proposed action, (Wistrom et al., 1989). In membranes, one would expect that proteins moving in and out of position within a monolayer, with varying lipid-protein interaction, would profoundly affect these in-plane interactions.

Molecular motions and molecular shapes

These molecular dimensions and their changes must eventually be interpreted in the light of the dynamics of the molecular configurations in the system. As time-averaged dimensions produced by highly mobile and conformationally dynamic molecules, these results give no indication of the variations that make up these averages. Conversely any model or measure of the molecular dynamics of these systems must account for or be consistent with the molecular dimensions described here. As an example, derivation of molecular lengths from the recently observed increase in isotropy of orientational order parameter in the L-H_{II} transition (for example, Lafleur et al., 1990; Thurmond et al., 1993) are sensitively dependent on molecular areas and pivotal positions.

The average area ratio A_t/A_p gives a good quantitative measure of a "shape" parameter for these molecules. However, Fig. 12, which shows only four possibilities of packing the same number of molecules into identical dimensions, taught us the futility of thinking about molecular shapes beyond these average area/ratios. These packings accommodate very different "shapes" of individual excluded volumes and are not mutually exclusive.

With no indication of the profile of the molecular areas, the kind of anisotropy giving rise to the very different principal radii of curvature in the H_{II} monolayer remains an enigma. The "ripple" phases of lipids represent structures of bilayers that have very different principal radii. One recent accounting of them couples molecular tilt to membrane curvature, a coupling that results from steric interactions between neighboring molecules (Lubensky and MacKintosh, 1993). In that gel state system the molecules are rigid but it may be possible that a similar approach could be applied to

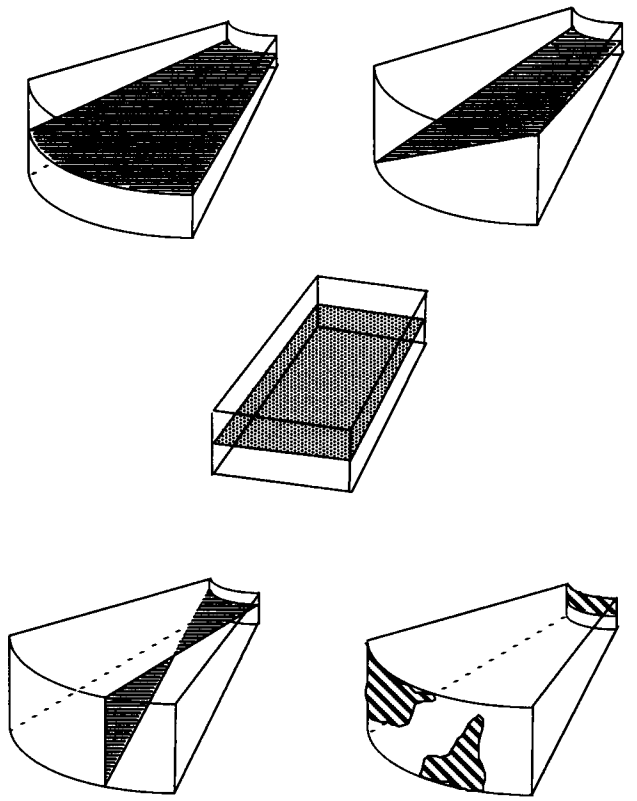

FIGURE 12 Schematic illustration showing some of many possibilities of packing two lipid molecules, separated by the stippled surfaces, into identical measured dimensions of a segment of the hexagonal phase and into a lamellar phase segment. The scheme illustrates the difficulty of translating the precisely measured, but globally averaged, areas and linear dimensions of the hexagonal structure into the details of packing a variety of dynamic molecular conformers. It also highlights the futility of using "shape" arguments to justify the geometry of molecular packing. Even in the lamellar phase there is little evidence that the whole molecules are symmetric about their long axis.

layers with disordered, fluid chains. It would appear to require molecules that are, on the appropriate time scale, rotationally asymmetric about their long axis. The single parameter that might measure that is the axial symmetry of the rotational diffusion of the whole molecule. While all indications are that internal motions of the molecule are symmetric about its long axis, whether the whole molecule, including correlations between the hydrocarbon chains, has rotational symmetry is not yet determined. While it has been assumed that such axial symmetry exists for molecules in the lamellar phase, that has not been established. It appears that this outstanding problem requires some new insight into how one can better dissect and measure the individual contributions to the internal free energy of these structures. It is hoped that the anomalous transition sequence and consequent structural changes reported here the might inspire such insight.

We acknowledge many useful discussions with Drs. Sergey Leikin and Adrian Parsegian.

This work was supported by the Natural Sciences and Engineering Research Council of Canada. R.P.R. is a Killam Research Fellow of the Canada Council.

REFERENCES

Boni, L. T., Stewart, T. P., and S. W. Hui. 1984. Alteration in phospholipid polymorphism by polyethylene glycol. *J. Membr. Biol.* 80:91–104

Charvolin, J. 1990. Crystals of fluid films. *Contemp. Phys.* 31:1–17

Fattal, D. R., and A. Ben-Shaul. 1993. A molecular model for lipid-protein interactions in membranes: the role of hydrophobic mismatch. *Biophys. J.* 65:1795–1809.

Gawrisch, K., V. A. Parsegian, D. A. Hajduk, M. W. Tate, S. M. Gruner, N. L. Fuller, and R. P. Rand. 1992. Energetics of a hexagonal-lamellar-hexagonal transition sequence in dioleoylphosphatidylethanolamine membranes. *Biochemistry.* 31:2856–2864.

Gruner, S. M. 1989. Hydrocarbon chain conformation in the H_{II} phase. *Biophys. J.* 56:1045–1049.

Helfrich, W. 1973. Elastic properties of lipid bilayers. Theory and possible experiments. *Z. Naturforsch.* 28C:693:703.

Hubner, W., and H. H. Mantsch. 1991. Orientation of specifically $^{13}C{=}O$ labeled phosphatidylcholine multilayers from polarized attenuated total reflection FT-IR spectroscopy. *Biophys. J.* 59:1261–1272.

Israelachvili, J. N., S. Marcelja, and R. G. Horn. 1980. Physical principles of membrane organization. *Q. Rev. Biophys.* 13:121–200.

Kirk, G. L., and S. M. Gruner. 1985. Lyotropic effects of alkanes and headgroup composition on the L_a-H_{II} lipid liquid crystal phase transition: hydrocarbon packing versus intrinsic curvature. *J. Phys.* 46:761–769.

Kirk, G. L., S. M. Gruner, and D. L. Stein. 1984. A thermodynamic model of the lamellar to inverse hexagonal phase transition of lipid membrane-water systems. *Biochemistry.* 23:1093–1102.

Kozlov, M. M., S. Leikin, and R. P. Rand. 1994. Energetics of the reentrant hexagonal-lamellar-hexagonal transition in phospholipids. *Biophys. J.* 66:A299.

Kozlov, M., and M. Winterhalter. 1991a. Elastic moduli for strongly curved monolayers. Position of the neutral surface. *J. Phys. France II.* 1: 1077–1084.

Kozlov, M., and M. Winterhalter, 1991b. Elastic properties of strongly curved monolayers. Analysis of experimental results. *J. Phys. France II.* 1:1085–1100.

Kozlov, M., M. Winterhalter, and D. Lerche. 1992. Elastic properties of strongly curved monolayers. Effect of electric surface charges. *J. Phys. France II.* 2:175–185.

Lafleur, M., P. R. Cullis, B. Fine, and M. Bloom. 1990. Comparison of the orientational order of lipid chains in the L_a and the H_{II} phases. *Biochemistry.* 29:8325–8333

Lerche, D., N. L. Fuller, and R. P. Rand. 1991. Membrane curvature and structural transitions for charged/uncharged phospholipid mixtures. *In* The Structure and Conformation of Amphiphilic Membranes. R. Lipowsky, D. Richter, and K. Kramer, editors. *Springer Proc. Phys.* 66:226–229.

Lubensky, T. C., and F. C. MacKintosh. 1993. Theory of "ripple" phases of lipid bilayers. *Phys. Rev. Lett.* 71:1565–1568.

Luzzati, V. 1968. The structure of the liquid-crystalline phases of lipid-water systems. *In* Biological Membranes. D. Chapman, editor. Academic Press, New York. 71–123.

Luzzati, V., and F. Husson. 1962. X-ray diffraction studies of lipid-water systems. *J. Cell. Biol.* 12:207–219.

Parsegian, V. A. 1972. Nonretarded van der Waals interaction between anisotropic long thin rods at all angles. *J. Chem. Phys.* 56:4393–4396.

Parsegian, V. A., N. L. Fuller, and R. P. Rand. 1979. Measured work of deformation and repulsion of lecithin bilayers. *Proc. Natl. Acad. Sci. USA.* 76:2750–2754.

Rand, R. P., N. L. Fuller, S. M. Gruner, and V. A. Parsegian. 1990. Membrane curvature, lipid segregation, and structural transitions for phospholipids under dual solvent stress. *Biochemistry.* 29:76–87.

Rand, R. P., and V. A. Parsegian. 1989. Hydration forces between phospholipid bilayers. *Biochim. Biophys. Acta.* 988:351–376.

Scherer, J. R. 1989a. Dependence of lipid chain and headgroup packing of the inverted hexagonal phase on hydration. *Biophys. J.* 55:965–972.

Scherer, J. R. 1989b. Reply to "Hydrocarbon chain conformation in the H_{II} phase." *Biophys. J.* 56:1047–1049.

Seddon, J. M. 1990. Structure of the inverted hexagonal (H_{II}) phase and non-lamellar phase transitions of lipids. *Biochim. Biophys. Acta.* 1031: 1–69.

Seddon, J. M., G. Cevc, R. D. Kaye, and D. Marsh. 1984. X-ray diffraction study of the polymorphism of hydrated diacyl- and dialkylphosphatidylethanolamines. *Biochemistry.* 23:2634–2644.

Seigel, D. P. 1993. Energetics of intermediates in membrane fusion: comparison of stalk and inverted micellar intermediate mechanisms. *Biophys. J.* 65:2124–2236.

Tate, M. W, and S. M. Gruner. 1989. Temperature dependence of the structural dimensions of the inverted hexagonal (H_{II}) phase of phosphatidylethanolamine-containing membranes. *Biochemistry.* 28:4245–4253.

Thurmond, R. L., G. Lindblom, and M. F. Brown. 1993. Curvature, order, and dynamics of lipid hexagonal phases studied by deuterium NMR spectroscopy. *Biochemistry.* 32:5394–5410.

Turner, D. C., and S. M. Gruner. 1991. X-ray diffraction reconstruction of the inverted hexagonal (H_{II}) phase in lipid-water systems. *Biochemistry.* 31:1340–1355.

Turner, D. C., and S. M. Gruner. 1992. X-ray diffraction of the inverted hexagonal (H_{ii}) phase in lipid-water systems. *Biochemistry.* 31:1340–1335.

Turner, D. C., S. M. Gruner, and J. S. Huang. 1992. Distribution of decane within the unit cell of the inverted hexagonal (H_{II}) phase of lipid-water-decane systems determined by neutron diffraction. *Biochemistry.* 31:1356–1363.

Wistrom, C. A., R. P. Rand, L. M. Crowe, B. J. Spargo, and J. H. Crowe. 1989. Direct transition of dioleoylphosphatidylethanolamine from lamellar gel to inverted hexagonal phase caused by trehalose. *Biochim. Biophys. Acta.* 984:238–242.